Si passivation effects on atomic bonding and electronic properties at HfO2/GaAs interface: A first-principles study

Weichao Wang, Ka Xiong, Cheng Gong, Robert M. Wallace, and Kyeongjae Cho

Citation: Journal of Applied Physics **109**, 063704 (2011); doi: 10.1063/1.3554689
View online: http://dx.doi.org/10.1063/1.3554689
View Table of Contents: http://scitation.aip.org/content/aip/journal/jap/109/6?ver=pdfcov
Published by the AIP Publishing

Si passivation effects on atomic bonding and electronic properties at HfO_2/GaAs interface: A first-principles study

Weichao Wang,[1] Ka Xiong,[1] Cheng Gong,[1] Robert M. Wallace,[1,2] and Kyeongjae Cho,[1,2,a)]
[1]*Department of Materials Science and Engineering, The University of Texas at Dallas, Richardson, Texas 75080, USA*
[2]*Department of Physics, The University of Texas at Dallas, Richardson, Texas 75080, USA*

(Received 16 July 2010; accepted 17 January 2011; published online 18 March 2011)

A theoretical study on atomic structures and electronic properties of the interface between GaAs and HfO_2 is reported. The intrinsic gap states are mainly originated from Ga dangling bonds, partial Ga-oxidation, and As−As dimers in the reconstructed interface structures. Si passivation interlayer can introduce two types of Si local bonding configuration of Si interstitial or substitutional defects (Si_{Hf}). Si_{Hf}–passivated interfaces are found to be energetically stable and can suppress the interfacial flat bandgap state stemming from partial Ga-oxidation into the valence band of bulk GaAs. Furthermore, gap states near the conduction bandedge are partially reduced. With the increase of Si concentration at the interface, the charge state of interfacial Ga decreases from +1.26 to between +0.73 and +0.80, and this change shows a Ga oxidation state transformation from Ga_2O_3 (+1.7) to Ga_2O (+0.52) states. The metastable Si interstitials also eliminate Ga_2O_3-oxidation state and creates Ga_2O-like Ga charge state at the interface. However, the gap states near the conduction bandedge cannot be passivated by substitutional (Si_{Hf}) nor by interstitial (Si_i) silicon. The detailed nature of the gap states examined in this modeling study would facilitate further development of interface passivation and the optimization of Si-passivation layers. © *2011 American Institute of Physics*. [doi:10.1063/1.3554689]

I. INTRODUCTION

GaAs has been of great interest as high performance channel material in metal-oxide-semiconductor field effect transistors (MOSFETs) because of its higher mobility and higher breakdown electric field compared to Si-based devices. The higher mobility leads to faster complementary MOS (CMOS) logic operation; higher breakdown field supports higher power/temperature applications; and band structure engineering would offer design flexibility. However, a major obstacle for integrating GaAs into MOS devices is the poor interface quality between channel and gate oxide leading to Fermi level pinning. The interface density of states (*Dit*) of GaAs/HfO_2 interface can be reduced to 10^{11} cm^{-2} eV^{-1} (Refs. 1 and 2). Compared to that of the Si/SiO_2 interface[3] (10^{10} cm^{-2} eV^{-1} or less), GaAs-induced Dit is still too high to be operable. A field effect transistor requires the gate field to be able to sweep the Fermi level across GaAs's bandgap to vary the carrier densities, and the poor interface quality requires higher gate voltage to unpin the Fermi level as well as reduces the device reliability. Intensive research effort has been devoted to investigate the origin of Fermi level pinning effect and to search for optimum passivation schemes to improve the interface quality.[4–7]

To gain an understanding on the interface gap state formation and the Fermi level pinning, GaAs surface electronic structures have been previously studied under oxidation conditions. Fermi level pinning[8] upon GaAs surface oxidation has been attributed to oxygen-induced displacement of surface As atoms[9,10] and As_{Ga} antisite defects.[9,11] Nevertheless, compared to GaAs surface, the high-*k*/GaAs interface is supposed to show a more complicated pinning mechanism due to many possible interface bonding configurations. Unlike the Si/SiO_2 interface with high thermal stability and low density of gap states due to the nature of partially covalent tetrahedral bonding Si−O, high dielectric constant (κ) oxides such as HfO_2 (Ref. 12) and Pr_2O_3 (Ref. 13) have primarily ionic bonding with variable atomic coordination numbers. Such ionic bonding in high-*k* dielectrics would lead to various Ga(As) oxides at the interface with different charge states of interfacial Ga and As. In GaAs side, Ga (As) has fractional charge of 0.75 (1.25 *e*), which make the Ga (As) bonds very hard to be passivated. Conventional Si/SiO_2 interface passivation method is not suitable for GaAs/high-*k* interface. Additionally, these various charge states cause many possible structural disorders such as dangling Ga (As) and As−As bonds so that a significant amount of interfacial gap states would be expected to be present. Consequently, the interfacial stability may be reduced; nevertheless, this problem could be decreased by introducing passivation layers such as Si into the interface. Besides the intrinsic complexity of the interface atomic structures, native oxides such as Ga_xO and As_xO and the interdiffusion of As and O may appear as well during the gate dielectric deposition.[14] As-oxides can be removed by HF and $(NH_4)OH$ surface treatments[15] or recently by atomic layer deposition (ALD).[16] Residual Ga−O bonding becomes very stable. It is therefore important to clarify the role of Ga atomic bonding at the interface. As this problem is not fully understood yet, many experimental efforts have been attempted to clarify the interface properties.[15–17] It has been reported that the Fermi level pining is due to the presence of the native oxide Ga_2O_3

a)Electronic mail: kjcho@utdallas.edu

(Ga^{3+}), and that the unpinning of the Ga_2O_3/GaAs system has been attributed to a Ga_2O/GaAs like interface in which the Ga and As surface atoms are restored to near-bulk charge states. We have recently found[18] has found that the gap states mainly arise from As−As dimers, Ga-O partial saturation, and Ga (As) dangling bonds. The subsequent analysis of charge transfer shows that the different interfacial Ga−O bonding drives various charge states of Ga such as 3+, 1+ and intermediate states. In addition, the As−As dimers and Ga (As) dangling bonds may occur due to the complicated nature of reconstructed interfacial bonding. Note that XPS data on GaAs/HfO_2 interface have shown As−As bonding in annealed samples which are consistent with the As−As dimer reconstruction in our model interface.[16–18] All these above structural disorders may be responsible for the interfacial gap states (Refs. 15–18).

Based on the experimental and theoretical understanding on the origin of gap states, some interfacial control layers such as Si, Ge, and Si/Ge are used in experimental studies to passivate GaAs related interfaces.[19–21] Using Si passivation layer, Hinkle *et al.*[17] found that the high charge state of interfacial Ga species (Ga^{3+}) was reduced to Ga^{+}. The reduction of the charge state of interfacial Ga species reflects the effect of Si passivation, as the frequency dispersion of capacitance faded when Ga_2O_3 (Ga^{3+}) is removed from the interface. However, the mechanism of this unpinning remains unexplained, as the physics behind the charge state change from 3+ to 1+ is unknown and the impact of other structural disorders is not clearly understood as well. Consequently, an understanding on the interfacial atomic bonding and the mechanism of Si passivation at the GaAs/HfO_2 interface is needed to elucidate the interface atomic and electronic properties.

For this purpose, we have performed first-principles density functional theory (DFT) study of GaAs-HfO_2 interface with controlled silicon passivation at the interface. This paper is organized as follows. In Sec. II, we discuss the computational method used in DFT calculations. In Sec. III, we first investigate the origin of gap states at the GaAs/HfO_2 interface. Second, the atomic bonding of GaAs/HfO_2 with Si passivation is explored with controlled atomic scale interface structures. In the third part, we focus on the stabilities of interfaces with various Si local bonding. In part four, we study the impact of Si passivation on the interfacial electronic properties. The last section is our conclusion.

II. COMPUTATIONAL METHODS

Our calculations are based on the density functional theory (DFT) method with the PW91 version of the generalized gradient approximation (GGA), as implemented in a plane-wave basis code VASP.[22] The pseudopotential is described by projector-augmented-wave (PAW) method.[23] An energy cutoff of 400 eV and an $8\times8\times1$ *k*-point with a Γ centered *k* mesh are used in our calculations. The ionic force is converged to 0.02 eV/Å in the atomic structure optimization.

We used a slab model of cubic HfO_2 on GaAs with Ga−O bonding at the interface since a stable interface terminated with Ga−O bonds was observed experimentally.[24] In this model, a 10 Å thick vacuum region without the dipole correction is adopted to avoid the interaction between the slab and its images. The bottom atomic layer of the slab (Ga) is passivated by pseudohydrogen to saturate the dangling bonds. Meanwhile, for the top atomic layer (HfO_2) of the slab, half of the oxygen atoms are removed to generate an insulating HfO_2 top surface. Thus, the passivation of the top (HfO_2) and bottom (GaAs) surfaces ensures that all the gap states originate from atomic interactions at the interface. The GaAs slab is 27.16 Å thick with 10 layers of Ga (40 Ga atoms) and 9 layers of As (36 As atoms), while the HfO_2 slab is 13.42 Å thick with 5 layers of Hf (25 Hf atoms) and 6 layers of O (55 O atoms). For the supercells of our interface models, the atomic positions are fully relaxed and the supercell length is re-optimized to GaAs lattice constant, and HfO_2 is strained less than 0.3%.

Since the bulk terminated surface of HfO_2 slab contains 10 O atoms in the model interface supercell, which is nonstoichiometric and represents the interface growth under oxygen rich condition, it is denoted as "O10" model interface. However, interfacial oxygen content varies with respect to ambient oxygen pressure during the oxide growth.[25] Formation energy versus oxygen chemical potential was investigated to study the stabilities of interfaces with various interfacial oxygen contents. It was found that O10 interface only exists at extreme O-rich condition based on our previous study.[18] Disregarding the extreme O-rich limit, interfaces with less interfacial oxygen atoms display higher stability than O10 interface. Specifically, interface O9 (nine O atoms at the interface) was found to be energetically favorable within a large range of oxygen chemical potential (49%) corresponding to experimental growth conditions.[18] In our present work, modeling study is focused on the O9 interface shown in Fig. 1(a).

Amorphous Si (*a*-Si) interlayer has been considered as a promising passivation candidate to provide a high-quality GaAs/HfO_2 interface.[26] At the atomic level, the Si atoms stay as either interstitial or substitutional defects at the interface. In the case of substitution, Si may substitute interfacial Ga (Si_{Ga}), As (Si_{As}), O (Si_O), and Hf (Si_{Hf}) sites. Our DFT energy calculation study demonstrates that Si_{Hf} is the most stable configuration, and only Si−O bonds can stably exist at the interface. Therefore, in this study we focus on investigating substitutional Si_{Hf} at the HfO_2/GaAs interface. In the case of Si interstitials (denoted as Si_i), the Si is introduced at various sites at the interface. For both interstitial and substitutional Si, we gradually increase Si content and investigate the impact of the Si concentration on the electronic structures and stability at the HfO_2/GaAs interface. For Si_{Hf}, we consider five configurations from one Si_{Hf} to five Si_{Hf} (which represent a full monolayer passivation) as in our supercell model each Hf layer contains five Hf atoms. For Si_i, we consider four configurations, one Si_i to four Si_i in which the number of Si is enough to show the passivation effect. In fact, more than four Si_i are more likely to produce crystalline Si behavior which induces tail states within GaAs gap, and therefore, interfaces with more than four Si_i is not included in the present work.

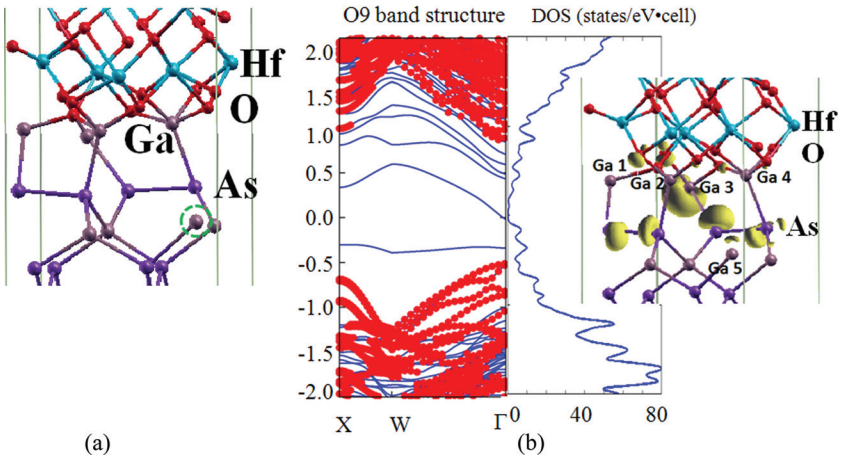

FIG. 1. (Color online) (a) Side view of GaAs:HfO_2 interface model (O9). (b) Left and center panels represent the band structures and total density of states of interface O9, respectively. The dotted region indicates the projected GaAs bulk band. The right inset in (b) shows the partial charge distribution within the bandgap of bulk GaAs. The Ga, As, Hf, and O atoms are depicted by light gray, purple, light blue, and red balls, respectively. Charge is in yellow. The electron density is 4.0×10^{-2} e Å^{-3}. Fermi level is set at 0 eV.

III. RESULTS AND DISCUSSION

A. Origin of intrinsic interface gap states

Figure 1(a) depicts the optimized GaAs/HfO_2 interface (O9 model) by the conjugate gradient (CG) method,[27] with a convergence of 0.01 eV/Å. At the interface, the Ga−O average bond length is 1.97 Å, which is close to that in bulk Ga_2O_3 (2.01 Å).[28] To determine the oxidation state of interfacial Ga, Bader charge decomposition method,[29] i.e., zero flux surfaces to divide atoms, is utilized to compute the atomic charge distribution. We applied the method to calculate charge states of interfacial Ga atoms. The average charge state of the interfacial Ga is +1.45 comparable to +1.70 of bulk Ga_2O_3 rather than +0.52 of bulk Ga_2O. Thus the interfacial Ga−O bonds have similar character to those in Ga_2O_3 which is consistent with what was found experimentally.[15–17] In these experimental works, only Ga-suboxides (i.e., Ga_2O_3) exist and As- related oxides are consumed by the atomic layer deposition (ALD) via a self-cleaning effect.[17] The relaxed structure [Fig. 1(a)] shows the reconstructed interface in which one Ga−As bond between the second (As) and the third top layers (Ga) of GaAs is broken and leaves a Ga dangling bond. Meanwhile, two As−As dimer pairs are formed resulting from the charge loss of the interfacial As atoms.

The left and center panels in Fig. 1(b) are the band structure and the total density of states (DOS) of O9 interface, respectively. The Fermi level is shifted to 0 eV. At Γ point in the band structure, there are six bands within the bulk bandgap of GaAs. In the lower half of the GaAs bandgap, there is a flatband that produces a high density of states [refer to the center panel of Fig. 1(b)] which can lead to Fermi level pinning. This flatband is induced by the interfacial Ga atom bonded to As and oxygen (e.g., Ga3). The gap states located in the upper half of GaAs bandgap show lower density of states than that in the lower half region and are induced by As−As dimers and Ga dangling bond [Ga5 in Fig. 1(b) inset]. The right inset in Fig. 1(b) describes partial charge distribution within the gap region of bulk GaAs, which clearly indicates that gap states arise from partial Ga-(Ga3) oxidation, two As−As dimers and a Ga dangling bond. Specifically, Ga1, Ga2, Ga3, and Ga4 all contribute gap states due to their partial oxidation. However, Ga1, Ga2, and Ga4's contribution to the gap states are much smaller than that of Ga3 so that only Ga3's contribution is clearly visible in Fig. 1(b) inset. In general, one should note that to obtain a high quality interface, interfacial As must be restored to its near-bulk charge state in GaAs. In addition, the Ga dangling bonds and the Ga-partial oxidation should be avoided as well. These considerations provide a clue on how to remove the gap states by different interface passivation strategies.

B. Atomic structures of Si_i and Si_{Hf} at HfO_2/GaAs interfaces

In this section, we discuss the detailed model approaches of developing silicon passivated GaAs/HfO_2 interfaces. Figure 2 shows the relaxed atomic structures of various passivated interfaces with Si_{Hf} and Si_i. Due to the nature optimization method to nearby local energy minimum, we consider as many defect configurations as practicable. For instance, in Fig. 2(a), there are five possible Si replacements of Hf sites in the interfacial Hf layer. All of the five configurations are optimized and only the one with lowest energy is considered in this study. Figure 2(a) exhibits the interface with one Si_{Hf} labeled as $1Si_{Hf}$. We have optimized all the five possible Si_{Hf} sites at the interface since there are five Hf atomic sites for Si to substitute. Figure 2(a) displays the most stable interface structure with one Si_{Hf}. Similarly, we placed Si at various sites for $2Si_{Hf}$, $3Si_{Hf}$, and $4Si_{Hf}$ based on the interface symmetry. The most stable configurations are given for each case in Figs. 2(b)−2(e). When Si_{Hf} increases from one to four as shown in Figs. 2(a)−2(d), we found that the two As−As dimers and one Ga dangling bond remain at the interface. However, the Ga dangling bond was removed in $5Si_{Hf}$ interface [Fig. 2(e)]. As a result, As−As dimmers still exist with a bond length of 2.60 Å. In all substitutional positions, the Si atom has nearly the same charge as in bulk SiO_2, which may indicate that the presence of nonsilicon second neighbors does not affect its bonds to neighboring oxygen atoms.

Figures 2(f)−2(i) show optimized atomic configurations with different amounts of Si_i at O9 interface. Interfaces are referred by the number of Si interstitials (e.g., one Si interstitial is denoted as $1Si_i$). For the $1Si_i$ interface (Fig. 2f), Si stays above one As−As dimer and forms As-Si and Si−O bonds leading to As-Si-As bond formation by breaking the As−As dimer. For two Si interstitials (i.e., $2Si_i$), there is no As−As dimer left due to the formation of As−Si−As bonds

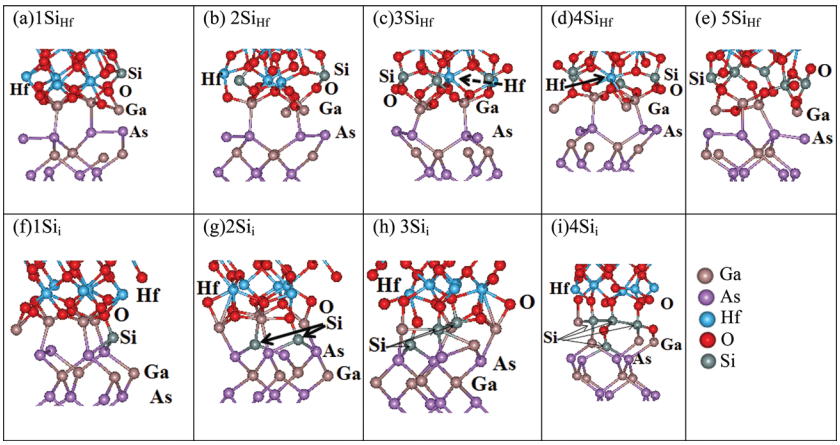

FIG. 2. (Color online) (a)−(e) depict side views of the interfaces with Si replacements of interfacial Hf from one to five, respectively. (f)−(i) Depict side views of the interfaces with Si interstitials from one to four, respectively. Ga, As, Hf, O, and Si atoms are represented by light gray, purple, light blue, red, and dark gray balls, respectively.

at both As−As dimer sites. The interstitial Si atoms have also formed Si−O and Ga−Si bonds as shown in Fig. 2(g). When one more Si_i is added into the interface [$3Si_i$ in Fig. 2(h)], the Si−Si bonding starts to form leading to a seed for metastable a-Si phase. The calculated Si−Si bond length is 2.37 Å, which is equivalent to that of bulk Si. Further addition of Si into $4Si_i$ interface [Fig. 2(i)] has formed more Si−Si bonds with an average bond length of 2.35 Å. In order to identify the bonding character of Si, we have calculated the atomic charge of Si, as shown in Table I. The charge states of Si in $1Si_i$, $2Si_i$, $3Si_i$, and $4Si_i$ are +1.04 e (2.96 e), +0.86 e (3.15 e), +1.24 e (2.76 e), and +1.26 e (2.74 e), respectively. Comparing the charge of Si in bulk SiO_2 (0.86 *e*, a quartz phase) and Si (4.00 *e*), interstitial Si approaches an intermediate suboxide state which is consistent with the Si local bonding configurations.

From the calculated atomic charge of the interfacial Ga (see Table I), we can see an increasing amount of charge transfer from Si to interfacial Ga. As the Si concentration increases, the charge state of interfacial Ga atom gradually decreases from +1.24 *e* to +0.59 *e*, which approaches the charge state of Ga in Ga_2O (+0.52 *e*). Therefore, the increasing amount of interstitial Si can help the $Ga_2O_3 \rightarrow Ga_2O$ transformation at the interface which is consistent with experimental observations.[17]

TABLE I. The average charge states of interfacial Ga and Si atoms for O9 and Si_i-passivated interfaces are listed. For Si_{Hf} interfaces, Ga3 charge state is presented. Si int. charge also depicts the average charge of interfacial Si atoms

Interfaces	Ga int. charge (+ *e*)	Si int. charge (+ *e*)
O9	1.24	
$1Si_i$	1.26	1.04
$2Si_i$	1.13	0.86
$3Si_i$	0.78	1.24
$4Si_i$	0.59	1.26
$1Si_{Hf}$	0.75	3.10
$2Si_{Hf}$	0.75	3.11
$3Si_{Hf}$	0.73	3.10
$4Si_{Hf}$	0.80	3.10
$5Si_{Hf}$	0.76	3.11
Bulk Ga_2O_3	1.70	
Bulk Ga_2O	0.52	

C. Formation energy of Si_{Hf} and Si_i

To investigate the thermodynamic stability of the interfaces, we have calculated the interface formation energies.[30] The lower interface formation energy represents more stable interface structure which is more likely form during the GaAs/HfO_2 gate stack growth. For a repeated slab structure, the interface formation energy can be expressed as

$$E_{\text{form}} = \frac{E_{\text{total}} - [nE_{\text{HfO}_2} + mE_{\text{Ga}} + p(E_{\text{GaAs}} - E_{\text{Ga}}) - qE_{\text{si}} \pm l\mu O]}{A} \quad (1)$$

where E_{total} is the total DFT energy of the interface supercell, n, m, q, and p are the numbers of HfO_2 bulk units, Ga, Si, and As atoms, and *l* is the number of excess/deficient (+/−) oxygen atoms (relative to HfO_2 stoichiometry). *A* is the interface area. E_{Ga} is the atomic energy of bulk Ga. The top and bottom surfaces of GaAs in the supercell is terminated by Ga, and we assume the growth of GaAs is under Ga-rich condition. E_{As} can be obtained by $E_{\text{As}} = E_{\text{GaAs}} - E_{\text{Ga}}$. The reference energy for pseudohydrogen (used to passivate the Ga bottom surface) is constant for all the interfaces, and thus this term is omitted in the formula without influencing the relative interface energies. For the chemical potential of Si at the interfaces, we have chosen bulk Si since bulk Si was used in experimental studies.[17] We have used the DFT total energies instead of the Gibbs free energies. We performed the calculation at 0 K temperature and thus the use of DFT energy would not significantly change the relative stability of different interface structures. It is necessary to define O chemical potential range since it is a variable indicating the HfO_2 growth condition in this study. We have assumed that the Hf bulk and O_2 gas reservoirs are in thermodynamic equilibrium with the HfO_2 thin film (unless the HfO_2 thin film would either grow or decompose). This condition requires

$$2\mu_O + \mu_{\text{Hf}} = E_{\text{HfO}_2}, \quad (2)$$

where E_X and μ_x are the DFT total energies and chemical potentials of unit *x*, respectively. The formation enthalpy (negative by convention) is defined as

$$E_{\text{HfO}_2} - (E_{\text{O}_2} + E_{\text{Hf}}) = H_{\text{f}}, \quad (3)$$

where E_{O2} and E_{Hf} are the DFT total energies per oxygen molecule and per Hf atom in bulk Hf, respectively. Because

of the fact that the chemical potential for each element cannot be larger than that of the bulk material (or gas element phase),[31] μ_o is constrained within the range of

$$\frac{1}{2}(E_{O_2} + H_f) \leq \mu_O \leq \frac{1}{2}E_{O_2}. \quad (4)$$

Once the range for the chemical potential of oxygen has been found (-10.39 eV $< \mu_O < -5.01$ eV), the interface formation energy can be expressed as a function of μ_o, using Eq.(1). For a typical atomic layer deposition (ALD) of HfO_2 upon GaAs, 600 K is normally applied.[17] Oxygen partial pressure is associated with oxygen chemical potential,[32,33] $\mu_O(T, P) = \mu_O(T, P^\circ) + 1/2KT \bullet \ln(P/P^\circ)$, where P and P° represent pressure at temperature T and 1 atm pressure, respectively. μ_O indicates oxygen chemical potential. In this case, 1 atm pressure approximately corresponds to -5.5 eV of O chemical potential.

Substitutional Si induces the strong Si−O bonds at the interfaces which help to increase the interface stability. Figure 3(a) shows that the $1Si_{Hf}$, $2Si_{Hf}$, $3Si_{Hf}$, $4Si_{Hf}$, and $5Si_{Hf}$ interface formation energies gradually decrease over the whole range of oxygen chemical potential relative to O9 interface. With the increasing of Si substitutional of Hf site, there are more Si−O bonds which are stronger than Hf−O. Consequently, the interfaces become more stable. This trend confirms the role of Si−O bonding in stabilizing the interface which indicates silicon suboxide or Hf silicate formation at the interface. Figure 3(b) shows the relative stabilities of the interfaces with different amount of Si interstitials. With increasing Si interstitials, the corresponding interface stability increases as shown in Fig. 3(b) inset. Note that $1Si_i$ interface is 0.005 eV/Å^2 less stable than O9 interface, but the formation energies of $2Si_i$, $3Si_i$, and $4Si_i$ interfaces decrease by 0.003 eV/Å,[2] 0.013 eV/Å^2, and 0.030 eV/Å^2 compared to O9 interface, respectively. Among all these four possible configurations, the $4Si_i$ interface is the most energetically favorable. Comparison of the interface energies of Si substitutional and intestinal defects clearly indicates that the Si substitution is thermodynamically more stable, and most interface silicon atoms would from Si suboxide or Hf silicate phases at the interface. However, it is worthwhile to note that the silicon is deposited as bulk *a*-Si on GaAs surface before HfO_2 growth in the experiments, and the kinetic barriers would leave some residual silicon bulk phase which corresponds to metastable Si interstitial interfaces (e.g., $3Si_i$ and $4Si_i$).

D. Passivation effects of Si_{Hf} and Si_i

To operate a field effect transistor, the gate field should be able to sweep the Fermi level across GaAs's bandgap and correspondingly vary the channel carrier density. However, if there are interface gap states (as shown in O9 interface), the Fermi level will be pinned, and the gate control will be lost or require higher voltage to operate. Hence it is necessary to reduce the interface state density by passivation with diverse elements, e.g., with amorphous Si interlayer. In this section, we will examine the interface gap states of thermodynamically stable Si-passivated interfaces (Si_{Hf}) as well as metastable interfaces (Si_i) which can be formed by kinetic constraint during the interface formation. We will examine the details of the interfacial electronic properties and clarify their passivation mechanisms.

Figure 4(a) shows the band structure (left panel) and the corresponding total density of states (center panel) of $5Si_{Hf}$ interface which is the most stable interface in our model study. The flatband (originating from Ga3 interface atom) in the lower half region of GaAs gap in O9 [Fig. 1(b)] is now suppressed into the valence band (VB) of bulk GaAs. Meanwhile, the gap states (originating from As−As dimers and Ga dangling bond) in the upper half of the bandgap are partially pushed into the GaAs conduction band (CB). Tail states right below the CB edge still remain, and this partial passivation effect could be explained by partial charge distribution at the interface [see Fig. 4(a) right inset]. Specifically, Si atoms have charge of ~0.89 *e* compared to ~1.67 *e* of Hf, and this different charge can stabilize the charge state of the interfacial Ga ("Ga3" in Fig. 1). Consequently, the corresponding interface gap states (in the lower half region of bulk GaAs gap) are suppressed into valence band region. In addition, based on the Bader charge analysis, As−As dimers gain limited charge compensation from Si as well as "Ga3" so that As−As related gap states are less stable and correspondingly partially pushed upward to the CB region.

The electronic structure of metastable $4Si_i$ interface is shown in Fig. 4(b). The flatband located in the lower half region of GaAs gap in O9 is removed by silicon interstitial atoms in the $4Si_i$ interface. In the upper half of the GaAs gap, there are three tail bands [Fig. 4(b)], and the charge density plot of the gap states reveals that these three tail bands originate from the interstitial Si and the Ga atoms. We found that the Ga atom has an excess charge of 0.22 e compared to that in bulk GaAs. This excess charge may adjust the local

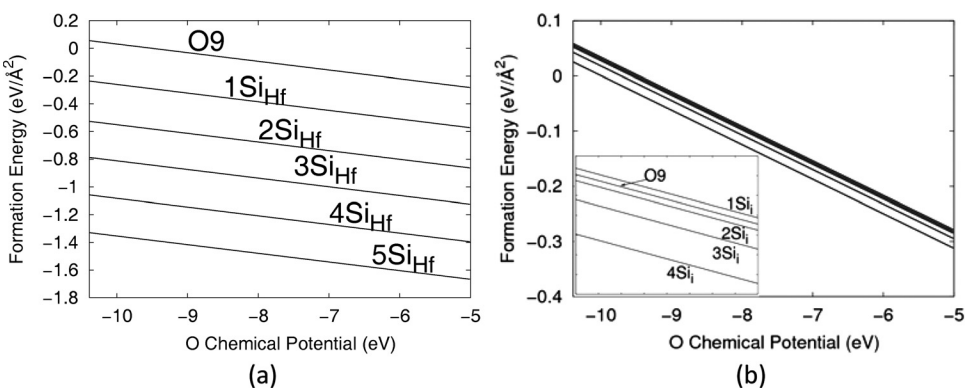

FIG.3. (a) and (b) are interface formation energies (E_{form}) of the various structures with Si_{Hf} and Si interstitials as a function of oxygen chemical potential (μ_o), respectively.

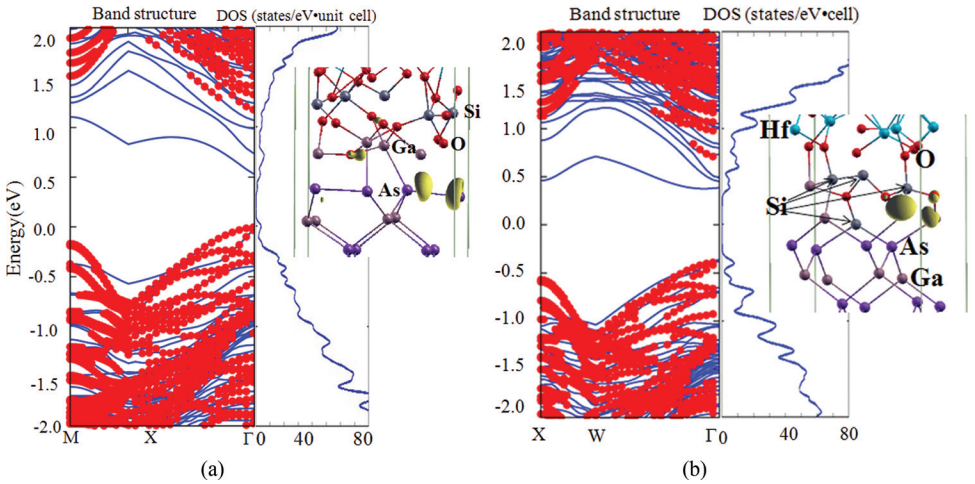

FIG. 4. (Color online) (a) and (b) Left and right panels represent the band structures and density of states (DOS) of the $5Si_{Hf}$ and $4Si_i$ interface, respectively. The dotted region indicates the projected GaAs bulk band. The inset figures of (a) and (b) depict the partial charge distribution plot of interfacial bands for the $5Si_{Hf}$ and $4Si_i$ interface, respectively. The electron density is 0.5×10^{-2} e Å^{-3} and 3.0×10^{-2} e Å^{-3}, respectively. The Ga, As, Hf, O, and Si atoms are depicted by light gray, purple, light blue, red, and dark gray balls, respectively. Charge density is in yellow. Fermi level is set at 0 eV.

bonding and produce interfacial gap states. The Si_i atoms behave like a bulk Si since interfacial Si−Si bonds remain 2.35 Å (comparable to that of bulk Si, 2.37 Å). Considering that Si has a smaller bandgap (1.12 eV) than GaAs (1.42 eV), the interfacial Si can contribute to the CB edge tail states, as shown in Fig. 4(b).

In Fig. 3, we have shown that the Si substitutional defects are thermodynamically more stable than the Si interstitials at the GaAs/HfO_2 interface. After examining the most stable substitutional and interstitial defects in Fig. 4, we now turn our attention to the effect of Si_{Hf} density on the interface gap states. Fig. 5 shows the comparison of total DOSs of the interfaces with increasing Si_{Hf} and O9 interface. For all the Si-passivated interfaces, the gap states close to VB maximum are removed, and the gap states within the upper half region is slightly shifted upward to CB edge. These DOS analysis clearly shows a partial passivation effect of silicon, but the gap states are not completely removed by increasing the Si-passivation density. This indicates that increasing Si amount at the interface is not helpful in removing gap states, and the $5Si_{Hf}$ interface actually shows slightly increased gap states compared to 1−3 Si_{Hf} interfaces. From the interface atomic structure analysis (shown in Fig. 2), the residual gaps states are contributed from As−As dimers and Ga dangling bonds.

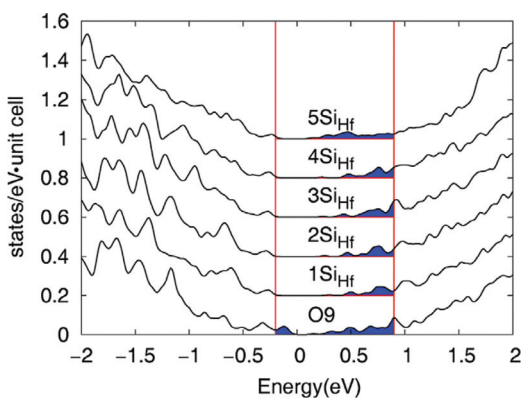

FIG. 5. (Color online) Comparison of normalized total density of states of the interfaces with increasing number of Si substitutional defects and O9 interface.

Experimentally,[17] frequency dispersion of capacitance versus gate voltage curves was observed with the existence of Ga atomic charges corresponding to Ga_2O_3 at the interface. This frequency dispersion could be eliminated by removing Ga atom in Ga_2O_3 state using Si passivation interlayer so that only Ga atoms corresponding to Ga_2O state would be present. This experimental observation could be explained by our Si-passivated Si_i and Si_{Hf} interface models. With the presence of Si interstitials or Si_{Hf} defects at the interface, the charge state of Ga decreases from +1.24 to +0.59 or +0.73-0.80 (see Table I), and this charge state change corresponds to the trend of experimentally assigned phase transformation from Ga_2O_3 to Ga_2O at the interface. Therefore, our model could explain the experimental findings[16,17] and provide an important insight on the nature of Si-passivation at high-k/$III-V$ interfaces.

IV. CONCLUSION

The atomic structures and electronic properties of the interfaces formed between GaAs substrate and HfO_2 gate dielectric are investigated by first-principles calculations. The O9 interface model shows that partially oxidized Ga atoms, As−As dimers and Ga dangling bonds occur at the optimized interface driven by charge redistributions of partially saturated interfacial bondings. These structural features of reconstructed O9 interface generate gap states to pin the Fermi level. In the study of Si passivation, Si_{Hf} interfaces show the better thermodynamic stability than Si interstitials at the interface, but the kinetic process of Si interlayer formation (from deposited a-Si layer) may leave some Si_i as metastable interface defects. The 1−5Si_{Hf} interfaces show increasing stability as the interfacial Si_{Hf} density increases, and all of them show the removal of the gap state originating from the interfacial Ga partial charge states (corresponding to the flatband located in the lower gap region of bulk GaAs). For these Si_{Hf} interfaces, As−As dimers remain in the optimized interface structures, and the gaps states in the upper region of GaAs bandgap are still present. In the study of the metastable Si_i interfaces, Si interstitials are also shown to remove the gap states near the VB edge by reducing the Ga oxidation state. Furthermore, As−As dimers and Ga

dangling bonds could be effectively removed by Si interstitials. However, Si−Si bonds are formed ($3Si_i$ and $4Si_i$) and additional gap states are introduced below the GaAs conduction bandedge. In summary, both types of interface Si-passivation are shown to remove the interface gap state near the VB edge, but there still remain the gap states near the CB edge. Finally, the density of state analysis has shown that the increasing the interfacial Si density does not correspondingly improve the interfacial gap states. These findings will provide a practical guidance for further investigation on the GaAs/HfO_2 interface passivation and experimental control of the interfacial Si density for optimal passivation.

ACKNOWLEDGMENTS

This research was supported by the FUSION/COSAR project and the FCRP Center on Materials, Structures, and Devices. We thank the *III−V* materials research group members at UTD for helpful discussions, in particular Prof. Eric Vogel and Prof. Christopher Hinkle. Calculations were done at the TEXAS ADVANCED COMPUTING CENTER (TACC).

[1]D. Shahrjerdi, M. Oye, A. Holmes, and S. Banerjee, Appl. Phys. Lett. **89**, 043501 (2006).
[2]V. Budhraja, X. Wang, and D. Misra, J. Mater Sci: Mater. Electron. **21**, 1322 (2010).
[3]Z. Jing, G. Lucovsky, and J. L. Whitten, J. Vac. Sci. Technol. B **13**, 1613 (1995).
[4]C. L. Hinkle, A. M. Sonnet, M. Milojevic, F. S. Aguirre-Tostado, H. C. Kim, J. Kim, R. M. Wallace, and E. M. Vogel, Appl. Phys. Lett. **93**, 113506 (2008).
[5]D. L. Winn, M. J. Hale, T. J. Grassman, A. C. Kummel, R. Droopad, and M. Passlack, J. Chem. Phys. **126**, 084703 (2007).
[6]I. Ok, H. Kim, M. Zhang, F. Zhu, S. Park, J. Yum, H. Zhao, and J. C. Lee, Appl. Phys. Lett. **91**, 132104 (2007).
[7]H. S. Kim, I. Ok, M. Zhang, C. Choi, T. Lee, F. Zhu, G. Thareja, L. Yu, and J. C. Lee, Appl. Phys. Lett. **88**, 252906 (2006).
[8]J. Tersoff, Phys. Rev. Lett. **52**, 465 (1984).
[9]M. J. Hale, S. I. Yi, J. Z. Sexton, A. C. Kummel, and M. Passlack, J. Chem. Phys. **119**, 6719 (2003).
[10]W. Wang, G. Lee, M. Huang, R. M. Wallace, and K. Cho, J. Appl. Phys. **107**, 103720 (2010)
[11]W. E. Spicer, Z. Liliental-Weber, E. Weber, N. Newman, T. Kendelewicz, R. Cao, C. McCants, P. Mahowald, K. Miyano, and I. Lindau, J. Vac. Sci. Technol. B **6**, 1245 (1988).
[12]E. Cho and K. J. Chang, Appl. Phys. Lett. **94**, 122901 (2009).
[13]A. Fissel, J. Dabrowski, and H. J. Osten, J. Appl. Phys. **91**, 8986 (2002).
[14]P. T. Chen, Y. Sun, E. Kim, P. C. McIntyre, W. Tsai, M. Garner, P. Pianetta, Y. Nishi, and C. O. Chui, J. Appl. Phys. **103**, 034106 (2008).
[15]J. C. Hackley, J. Derek Demaree, and T. Gougousi, Appl. Phys. Lett. **92**, 162902 (2008).
[16]F. S. Aguirre-Tostado, M. Milojevic, K. Choi, H. C. Kim, C. L. Hinkle, E. M. Vogel, J. Kim, T. Yang, Y. Xuan, P. D. Ye, and R. M. Wallace, Appl. Phys. Lett. **93**, 061907 (2008).
[17]C. L. Hinkle, M. Milojevic, B. Brennan, A. M. Sonnet, F. S. Aguirre-Tostado, G. J. Hughes, E. M. Vogel, and R. M. Wallace, Appl. Phys. Lett. **94**, 162101 (2009).
[18]W. Wang, K. Xiong, R. M. Wallace, and K. J. Cho, J. Phys. Chem. C **114**(51), 22610 (2010).
[19]H. Kim, I. Ok, M. Zhang, T. Lee, F. Zhu, L. Yu, and J. C. Lee, Appl. Phys. Lett. **89**, 222903 (2006).
[20]S. Tiwari, S. L. Wright, and J. Batey, IEEE Electron Device Lett. **9**, 499 (1988).
[21]H. Kim, I. Ok, M. Zhang, F. Zhu, S. Park, J. Yum, H. Zhao, J. C. Lee, J. Oh, and P. Majhi, Appl. Phys. Lett. **92**, 102904 (2008).
[22]G. Kresse and J. Furthmüller, Comput. Mater. Sci.**6**, 15 (1996); G. Kresse and J. Furthmüller, Phys. Rev. B **54**, 11169 (1996); G. Kresse and J. Hafner, Phys. Rev. B **47**, 558 (1993).
[23]P. E. Blochl, Phys. Rev. B **50**, 17953 (1994).
[24]C. L. Hinkle, A. M. Sonnet, E. M. Vogel, S. McDonnell, G. J. Hughes, M. Milojevic, B. Lee, F. S. Aguirre-Tostado, K. Cho, H. C. Kim, J. Kim, and R. M. Wallace, Appl. Phys. Lett. **92**, 071901 (2008).
[25]J. Park, M. Cho, S. K. Kim, T. J. Park, S. W. Lee, S. H. Hong, and C. S. Hwang, Appl. Phys. Lett. **86**, 112907 (2005).
[26]S. J. Koester, E. W. Kiewra, Y. Sun, D. A. Neumayer, J. A. Ott, M. Copel, and D. K. Sadana, D. J. Webb, J. Fompeyrine, J.-P. Locquet, C. Marchiori, M. Sousa, and R. Germann, Appl. Phys. Lett. **89**, 042104 (2006).
[27]W. H. Press, B. P. Flannery, S. A. Teukolsky and W. T. Vetterling, *Numerical Recipes* (Cambridge University Press, New York, 1986).
[28]S. Yoshioka, H. Hayashi, A. Kuwabara, F. Oba, K. Matsunaga and I. Tanaka, J. Phys.: Condens. Matter **19**, 346211 (2007).
[29]G. Henkelman, A. Arnaldsson, and H. Jónsson, Comput. Mater. Sci., **36**, 354 (2006).
[30]S. B. Zhang and John E. Northrup, Phys. Rev. Lett. **67**, 2339 (1991).
[31]G. X Qian, R. M. Martin, and D. J. Chadi, Phys. Rev. B **38**, 7649 (1988).
[32]S. Monaghan, J. C. Greer, and S. D. Elliott, Phys. Rev. B **75**, 245304 (2007).
[33]K. Reuter and M. Scheffler, Phys. Rev. B **65**, 035406 (2001).